

Examination of Indoor Localization Techniques and Their Model Parameters

Waltenegus Dargie and Jianjun Wen

Faculty of Computer Science, Technische Universität Dresden, 01062 Dresden, Germany

Email: {waltenegus.dargie, jianjun.wen}@tu-dresden.de

Abstract—The future, in which mobile robots and human beings intermingle in industrial complexes, shopping malls, airports, and similar areas, is not far. The condition, however, requires the realization of several features, including self-localization, self-navigation, identification and avoidance of obstacles, and dynamic route discovery. Indoor localization has been the subject of interest for over two decades, most recent advances attempting to take advantage of freely available signals from a plethora of indoor sources. As far as the estimation task is concerned, most of the models employ extended kalman filters and particle filters. Each technique has its own merits and demerits, as well as a set of assumptions. The purpose of this paper to identify the most significant components of these techniques and to closely examine the prevailing assumptions underlying the selection process of indoor localization techniques. Moreover, the paper experimentally demonstrates the error modeling process in kalman and particle filters.

Index Terms—Indoor localization, IMU, UWB, mobile robots, recursive filters, Kalman filter, particle filter, Bayesian Estimation, Importance Sampling

I. INTRODUCTION

A future in which mobile robots and human beings intermingle inside industrial complexes, shopping malls, airports, and similar spaces, with the robots carrying out many everyday tasks unassisted, is not far off. This scenario, however, is dependent on the realization of several features, including self-localization, self-navigation, identification and avoidance of obstacles, and dynamic route discovery.

Indoor localization has been the subject of interest for over two decades, with the most recent advances attempting to take advantage of (1) freely available signals from a plethora of indoor sources, (2) the availability of cloud/edge resources enabling the computation of a vast amount of data, and (3) a wide range of libraries implementing several recursive filters as well as unsupervised/deep learning algorithms.

Nevertheless, the success of indoor localization depends on various factors, including the underlying assumptions as regards the movement pattern and speed of the mobile robots and the sources delivering the raw data and their statistical dependence. The most widely employed estimation techniques are recursive filters whose foundation is to be found on Bayesian Estimation. One of their advantages is the ease with which they combine evidence. The purpose of this paper is to closely examine the theoretical basis of these approaches, the underlying assumptions they make as regards the raw data, and the most important model parameters and where they come

from. Throughout this paper, where it is not stated explicitly, the underlying context is the localization of mobile robots.

The remaining part of the paper is organized as follows: In Section II, we discuss the most important assumptions in employing recursive filters. In Section III, we discuss the reduction of uncertainty being one of the prevailing goals of any estimation assignment. In Section IV, we discuss the theoretical basis of recursive filters and highlight their similarities and differences. In Section V, we discuss the significance of model parameters and illustrate how they can be produced. In Section VI, we demonstrate how self-navigation can be realized by combining prediction and measurement using a Kalman filter. In Section VII, we review related work. Finally, in Section VIII, we provide concluding remarks and outline future work.

II. ASSUMPTIONS

The actual position of the robot we wish to localize cannot be known in a deterministic sense. Therefore, we have to begin the estimation process with a set of assumptions. From the outset, this task is bound by two opposing conditions. On the one hand, the more liberal we are with our assumptions, the simpler is the task, but the bigger will be our uncertainty. On the other hand, the stricter our assumptions, the more complex will be the mathematical expressions describing the estimation process. At this point one may ask: If the actual position of the robot is hidden from our sight, how can we ever know that our estimation is good enough? The answer to this question makes up the first fundamental assumption. We assume that there is a reference measurement system in place with respect to which we can measure the accuracy of our estimation. For example, in determining the robot's position, we can take a simple ruler as the reference measurement system.

The next two assumptions without which no estimation can be made are the following:

- The robot does not make arbitrary movements. In other words, there is a correlation between its past, present, and future locations. The significance of this assumption is that predictions can be made as regards its future locations. We depict this as a random variable, $x_p(t)$.
- The measurement we make reflects to a certain extent the actual position of the robot. We say “to a certain extent” because of the inherent imperfection of the measurement apparatus or setup as a result of which there is some

error associated with it. Hence, the measurement, too, is regarded as a random variable, $x_m(t)$.

Since $x_p(t)$ and $x_m(t)$ are random variables, we need their probability density functions to fully describe them. In Section V, we shall illustrate how they can be established. There is a one-to-one correspondence between a random variable and its probability density function (pdf). Therefore, reasoning about a random variable amounts to reasoning about its probability density, and vice versa. In probabilistic estimation, it is easier to begin with the pdf. The location with the highest probability is taken to be the location of the robot.

The fourth assumption is that $x_p(t)$ and $x_m(t)$ are statistically independent. This is because the prediction made prior to t is unaffected by the measurement taken at time t . Similarly, at time t , one can pick any measurement device, so that the measurement is not influenced by the prediction made prior to t . The usefulness of this observation is that in the probability space, the probability that the two random variables point to one and the same location can be expressed as:

$$p(x_p(t), x_m(t)) = p(x_p(t))p(x_m(t)) \quad (1)$$

Suppose $x_p(t)$ and $x_m(t)$ are both normally distributed random variables, centered at the actual location of the robot, say, θ . Furthermore, suppose also that the two have the same variance (this assumption is made only for the sake of illustration). Thus, we have,

$$p(x_p(t)) = \frac{1}{\sqrt{2\pi\sigma^2}} e^{-(x_p(t)-\theta)^2/2\sigma^2} \quad (2)$$

Likewise,

$$p(x_m(t)) = \frac{1}{\sqrt{2\pi\sigma^2}} e^{-(x_m(t)-\theta)^2/2\sigma^2} \quad (3)$$

The joint density function is:

$$p(x_p(t), x_m(t)) = \frac{1}{(2\pi\sigma^2)} e^{-\sum_{i=1}^2 ((x_i(t)-\theta)^2/2\sigma^2)} \quad (4)$$

where $x_1(t) = x_p(t)$ and $x_2(t) = x_m(t)$. Having the joint density function in place, we can now determine the best estimation strategy by differentiating Equation 4 with respect to θ , because we are interested in the value of θ which results in the highest probability. Alternatively, we can differentiate the logarithmic value of Equation 4 (due to the linearity property of logarithm). Thus, we have:

$$\ln \{p(x_p(t), x_m(t))\} = \ln(2\pi\sigma^2) - \sum_{i=1}^2 \frac{(x_i(t) - \theta)^2}{2\sigma^2} \quad (5)$$

Differentiating Equation 5 with respect to θ and setting the result to zero yields:

$$\hat{\theta}(t) = \frac{1}{2} \sum_{i=1}^2 x_i(t) \quad (6)$$

From Equation 6, we see that the assumptions of statistical independence and normal distributions lead to a linear estimation.

Type	Source	Time invariant?
e_r	Driving setup error	No
e_m	Measurement setup error	No
$e_p(t)$	Prediction error	Yes
$e(t)$	Overall estimation error	Yes

TABLE I
SUMMARY OF THE ESTIMATION ERRORS

III. UNCERTAINTY

In our endeavor to estimate the actual position of a robot, we are confronted with different types of uncertainties. The first arises from the imperfection of the robot's driving setup. If, for example, we configure the robot to travel at a speed of 1.5 m s^{-1} along the x-axis, it travels neither at this speed nor along the x-axis precisely. Therefore, in expressing the future position in terms of the present, we have to add an uncertainty term in the form of a random variable:

$$x(t+1) = \Phi x(t) + e_r \quad (7)$$

The term Φ , which, for our case is 1.5 m s^{-1} , is a connecting term and is not a probabilistic term. It is important to remark that e_r has nothing to do with the quality of the estimation technique.

The second type of uncertainty is due to the error introduced by the measurement setup:

$$x_m(t) = x(t) + e_m \quad (8)$$

This error, too, has nothing to do with the estimation technique. The third uncertainty, however, arises from the fact that we make estimation of $x(t)$ and all future predictions based on uncertain inputs and a set of assumptions which guide the selection of the estimation technique. Thus, we have:

$$x_p(t) = x(t) + e_p(t) \quad (9)$$

and,

$$\hat{x}(t) = x(t) + e(t) \quad (10)$$

where $\hat{x}(t) = f(x_p(t), x_m(t))$ is the best estimation we have of $x(t)$ and its accuracy and precision depend on the quality of the estimation technique. Notice that e_r and e_m are not functions of time, because the former depends on the robot's driving setup whereas the latter depends on the measurement setup. Table I summarizes all the errors one deals with during estimation.

A. Estimation Uncertainty

The aim of any estimation endeavor is to achieve two goals:

- To approach the true value; and,
- in doing so, to reduce the associated estimation variance.

These two aspects are often expressed in terms of accuracy and precision. The first goal is achieved when the expected value of our estimation aligns with the true value. The second goal is achieved by reducing the variance of the estimated random variable. Consider Equation 6. Whereas we started off by saying that the actual position of the robot at time t is θ , a fixed value, where we arrived at is, however, $\hat{\theta}(t)$, which is

a random variable. This is because the inputs we used for our estimation are random variables and any function of a random variable is by definition a random variable.

One way of evaluating whether our estimation endeavor has been successful is to quantify the extent to which these two goals are achieved. Equation 6, for example, fulfills these goals, because:

$$E[\hat{\theta}(t)] = \frac{1}{2}E\left[\sum_{i=1}^2 \mathbf{x}_i(t)\right] = \frac{1}{2}\sum_{i=1}^2 E[\mathbf{x}_i(t)] = \theta \quad (11)$$

Similarly, the variance of $\hat{\theta}(t)$ can be determined as follows:

$$\sigma_{\hat{\theta}}^2 = E\left[\left(\hat{\theta}(t) - \theta\right)^2\right] = \frac{1}{4}E\left[\left(\sum_{i=1}^2 (\mathbf{x}_i(t) - \theta)\right)^2\right] \quad (12)$$

Notice that in order to include θ into the summation term, we have to divide it by 2 because it will be added 2 times as a part of the summation term. The square of the summation term yields the following:

$$\sigma_{\hat{\theta}}^2 = \frac{1}{4}\sum_{i=1}^2 E[(\mathbf{x}_i(t) - \theta)^2] + \frac{1}{4}\sum_{i=1}^2 \sum_{j=1, j \neq i}^2 E[\mathbf{x}_i(t) - \theta] E[\mathbf{x}_j(t) - \theta]$$

The last term of the above expression is zero, because $x_p(t)$ and $x_m(t)$ are independent. Therefore, we conclude that:

$$\sigma_{\hat{\theta}}^2 = \frac{1}{4}\sum_{i=1}^2 E[(\mathbf{x}_i(t) - \theta)^2] = \frac{1}{4}\sum_{i=1}^2 \sigma_i^2 \quad (13)$$

Given the assumption that both inputs have the same variance:

$$\sigma_{\hat{\theta}}^2 = \frac{1}{4}\sum_{i=1}^2 \sigma^2 = \frac{\sigma^2}{2} \quad (14)$$

As can be seen, as a result of the linear combination, we reduced our uncertainty by half. In general, if we have n independent sources,

$$\lim_{n \rightarrow \infty} \frac{1}{n^2} \sum_{i=1}^n \sigma^2 = 0 \quad (15)$$

B. The Role of Variance in Estimation

The variance of an input random variable encodes our uncertainty in the random variable. Therefore, our confidence in the random variable should be inversely proportional to it. But confidence is a relative term. If two or more inputs are being considered during an estimation, the weight we attach to each input should also reflect the relative aspect of our confidence (often in the form of a normalization term). Suppose $x_p(t)$ and $x_m(t)$ have different variances in Equations 2 and 3. In which case, our best estimation can be expressed as:

$$\hat{\theta}(t) = \left[\frac{\sigma_m^2}{\sigma_p^2 + \sigma_m^2}\right] x_p(t) + \left[\frac{\sigma_p^2}{\sigma_p^2 + \sigma_m^2}\right] x_m(t) \quad (16)$$

provided that:

$$\left[\frac{\sigma_m^2}{\sigma_p^2 + \sigma_m^2}\right] + \left[\frac{\sigma_p^2}{\sigma_p^2 + \sigma_m^2}\right] = 1 \quad (17)$$

The linear combination reflects the confidence we attach to the two inputs. If σ_p^2 is larger than σ_m^2 , then we should give more weight to $x_m(t)$ and vice versa. Since:

$$\frac{\sigma_m^2}{\sigma_p^2 + \sigma_m^2} = 1 - \frac{\sigma_p^2}{\sigma_p^2 + \sigma_m^2}$$

Equation 16 can be reformulated as:

$$\hat{\theta}(t) = x_p(t) + K[x_m(t) - x_p(t)] \quad (18)$$

where:

$$K = \frac{\sigma_p^2}{\sigma_p^2 + \sigma_m^2} \quad (19)$$

Equation 19 is the fundamental expression of the kalman filter [1]. Logically, we can interpret it as follows: At first the robot has only $x_p(t)$ to rely on, because the prediction was made at time $t-1$. When, however, the measurement arrives, it doesn't have to do the estimation all over again; instead, it takes the difference between $x_m(t)$ and $x_p(t)$, scales this difference appropriately, and adds it to its existing knowledge. If there is no difference between these two, the robot trusts its prediction more and more in the future by updating its scaling factor, K .

IV. RECURSIVE ESTIMATION

Most existing indoor localization techniques mix $x_p(t)$ and $x_m(t)$ recursively. Besides reducing the computation cost, this approach enables to establish $x_p(t)$ from the best available evidence at $t-1$. As we have demonstrated in Equation 1, the independence assumption enables to mix the two in the probability domain. In this case, establishing the joint probability density function is the primary goal of recursive estimations. If, on the other hand, further assumptions can be plausibly made, then the raw measurements can be mixed directly. For example, statistics pertaining to the measurement setup can be established and verified independent of the estimation technique. More often than not, measurement devices (sensors) have zero mean, normally distributed errors. The kalman filter and its variants mix $x_p(t)$ and $x_m(t)$ directly by first determining the optimal mixing coefficient, $K(t)$, whereas other techniques, such as particle filters and Hidden Markov Models mix evidence in the probability domain.

A. Kalman Filter

In our initial derivation of the kalman filter (Equation 18), we expressed the scaling factor K as if it were independent of time, whereas $x_p(t)$ and $x_m(t)$ are functions of time. Particularly, the error contained in $x_p(t)$ accumulates over time and this aspect should be reflected in K . Hence, the mean square cumulative error at time t is expressed as:

$$C(t) = E[e^2(t)] \quad (20)$$

Variable	Explanation
$K(t)$	The Kalman constant for t
$x_m(t)$	Measurement
$x_p(t)$	Prediction
$x(t)$	Hidden (unknown) variable
$\hat{x}(t)$	The best estimation of $x(t)$
Φ	Factor connecting $x(t)$ and $x(t+1)$
$P(t)$	$E[(x(t) - x_p(t))^2]$
R	$E[e_m^2]$
Q	$E[e_r^2]$
$C(t)$	$E[(x(t) - \hat{x}(t))^2]$

TABLE II

SUMMARY OF THE KALMAN FILTER FORMULATION

Expressing the estimated position in terms of the predicted and measured positions and substituting $x_m(t)$ with $x(t) - e_m$ yields:

$$C(t) = [1 - K(t)]^2 E[(x(t) - x_p(t))^2] - K^2(t)E[e_m^2] \quad (21)$$

The term $E[(x(t) - x_p(t))^2]$ is the variance of $x_p(t)$. We denote it with $P(t)$, so that Equation 21 can be expressed in terms of it:

$$C(t) = (1 - K(t))^2 P(t) + K^2(t)R \quad (22)$$

where $R = E[e_m^2]$.

We are now in a position to choose the optimal $K(t)$ that minimizes our uncertainty – as discussed in Section III – at time t . This can be done by differentiating Equation 22 with respect to $K(t)$ and setting the result to zero. The result is:

$$K(t) = \frac{P(t)}{P(t) + R} \quad (23)$$

Equation 23 is similar to Equation 18, the only difference is that the prediction error covariance is expressed as a function of time. We will appreciate the significance of this shortly. Substituting Equation 23 into Equation 22 reduces the expression for $C(t)$ into:

$$C(t) = (1 - K(t)) P(t) \quad (24)$$

Our prediction of the robot's future position should include all the uncertainties accumulated thus far, namely,

$$\begin{aligned} x(t+1) &= \Phi x(t) + e_r \\ x_p(t+1) &= \Phi \hat{x}(t) \end{aligned} \quad (25)$$

Thus, the prediction error for $t+1$ is given as,

$$\begin{aligned} e_p(t+1) &= x(t+1) - x_p(t+1) \\ &= \Phi x(t) + e_r - \Phi \hat{x}(t) \\ &= \Phi e(t) + e_r \end{aligned} \quad (26)$$

The mean square prediction error for time $t+1$ is:

$$P(t+1) = \Phi^2 E[e^2(t)] + E[e_r^2] = \Phi^2 C(t) + Q \quad (27)$$

where $Q = E[e_r^2]$. With $P(t)$, $C(t)$, and $P(t+1)$ the Kalman Filter connects the past, the present, and the future. Tab. II summaries the most important Kalman notations.

B. Bayesian Estimation

The Baye's theorem, one of the most profound theorems in probability, is analogs to the inverse relation in mathematics. In Section II, we assumed that $x_p(t)$ and $x_m(t)$ are causally related with the hidden variable $x(t)$. This means that the converse is also true. Using Baye's theorem this can be expressed as:

$$p(x(t)|x_m(t), x_p(t)) = \frac{p(x(t), x_p(t), x_m(t))}{p(x_p(t), x_m(t))} \quad (28)$$

Considering the statistical independence, Equation 28 can be simplified into:

$$p(x(t)|x_m(t), x_p(t)) = p(x_p(t)|x(t)) p(x_m(t)|x(t)) p(n(t)) \quad (29)$$

where:

$$p(n(t)) = \left[\frac{p(x(t))}{p(x_p(t)) p(x_m(t))} \right]$$

Equation 29 is in essence the same as Equation 1. To appreciate the difference, though, suppose we observed a robot moving along the x-axis, taking off from x_0 and being at the locations $x_1, x_2, \dots, x_{t-1}, x_t$ at the time instances $1, 2, \dots, t-1, t$, respectively. The probability of observing the robot in this sequence can be described by the joint probability density function:

$$p(X_{0:t}) = p(x_0, x_1, \dots, x_t) \quad (30)$$

Equation 30 can be simplified using conditional probability. If we assume that the location of the robot at time t is independent of all its past locations save the location at $t-1$, we rewrite Equation 30 as:

$$p(X_{0:t}) = \prod_{i=1}^t p(x_i|x_{i-1}) \quad (31)$$

where x_0 is the initial position of the robot having a pdf of $p(x_0)$. As can be seen, Equation 31 establishes the basis for making predictions, for it says that the robot's transition from x_{t-1} to x_t is governed by the conditional probability density function $p(x_t|x_{t-1})$. Similarly, the measurement probability density function associated with $x(t)$ can be expressed as a conditional probability: $p(z(t)|x(t))$ or more simply as $p(z_t|x_t)$. This probability density is independent of both past and future measurements as well as locations.

With these in place the Bayesian Estimation expresses the probability of the robot having been at locations $X_{0:k}$ given all the evidence thus far as:

$$p(X_{0:t}|D_t) = \frac{p(D_t|X_{0:t}) p(X_{0:t})}{p(D_t)} \quad (32)$$

where $D_t = (z_1, z_2, \dots, z_t)$. Taking advantage of the expression:

$$p(D_t|X_{0:t}) = p(z_t, D_{t-1}|X_{0:t})$$

and expressing it conditionally as

$$p(z_t, D_{t-1}|X_{0:t}) = p(z_t|D_{t-1}, X_{0:t}) p(D_{t-1}|X_{0:t})$$

Because of independence:

$$p(z_t, D_{t-1} | X_{0:t}) = p(z_t | x_t) p(D_{t-1} | X_{0:t-1}) \quad (33)$$

Putting everything together, we have:

$$p(X_{0:t} | D_t) = \frac{p(z_t | x_t) p(x_t | x_{t-1}) p(D_{t-1} | X_{0:t-1}) p(X_{0:t-1})}{p(z_t | D_{t-1}) p(D_{t-1})} \quad (34)$$

But the last expression is $p(X_{0:t-1} | D_{t-1})$ so that we can rewrite Equation 34 as:

$$p(X_{0:t} | D_t) = \frac{p(z_t | x_t) p(x_t | x_{t-1})}{p(z_t | D_{t-1})} p(X_{0:t-1} | D_{t-1}) \quad (35)$$

Equation 35 gives expression to all the evidence we have up to time t , namely, to

- the freshly available measurement in the form of $p(z_t | x_t)$.
- the prediction in terms of $p(x_t | x_{t-1})$; and,
- the best evidence we had up to time $t - 1$ in terms of $p(X_{0:t-1} | D_{t-1})$.

Furthermore, it does not make any assumption as to the nature of these probability density functions.

Alternatively, we can limit our interest only to the current location of the robot given all the evidence we have so far, namely, to $p(x_t | D_t)$:

$$p(x_t | D_t) = \frac{p(D_t | x_t) p(x_t)}{p(D_t)} \quad (36)$$

We can express $p(D_t | x_t)$ as $p(z_t, D_{t-1} | x_t)$ or as

$$p(z_t | D_{t-1}, x_t) p(D_{t-1} | x_t)$$

Taking advantage of independence, the above expression reduces to:

$$p(D_t | x_t) = p(z_t | x_t) p(D_{t-1}) \quad (37)$$

Similarly, we can express $p(x_t)$ as:

$$p(x_t) = \int p(x_t | x_{t-1}) p(x_{t-1}) dx_{t-1} \quad (38)$$

Equation 38 says that the robot may arrive at x_t coming from infinite previous locations and each previous location has its own probability. In other words, Equation 38 is a prediction term. We can label it as $p(x_t | D_{t-1})$. Combining Equations 37 and 38 yields:

$$p(x_t | D_t) = \frac{p(z_t | x_t) p(x_t | D_{t-1})}{p(z_t | D_{t-1})} \quad (39)$$

Equation 39 says that the current location of the robot can be expressed in terms of the freshly available measurement – $p(z_t | x_t)$ and the prediction components.

C. Particle Filter

Nevertheless, Equations 35 and 39 are difficult to evaluate. For instance, in Section III, we mentioned that one way of evaluating whether our estimation endeavor is successful is to examine the expected value and the variance of the best estimation, $\hat{x}(t)$, both of which require the integration of a probability density function. So, if we take Equation 39 to

Variable	Explanation
D_t	A sequence of measurements up to t $D_t = (z_1, \dots, z_t)$
$x_{0:t}$	A sequence of hidden states (locations) $x_{0:t} = (x_0, x_1, \dots, x_t)$
$p(D_t)$	$p(z_1, z_2, \dots, z_t)$
$P(x_{0:t} D_t)$	posterior pdf associated with \hat{x}
$p(z_t x_t)$	Measurement probability – $p(x_m(t))$
$p(x_t D_{t-1})$	Prediction pdf
$p(x_t x_{t-1})$	Transition pdf

TABLE III

SUMMARY OF THE BAYESIAN ESTIMATION FORMULATION

be our probability density function, the mean of our best estimation is:

$$E[\hat{x}_t] = \int x_t p(x_t | D_t) dx_t \quad (40)$$

For most practical purposes, it suffices to approximate the integration by summation, by drawing a large number of samples from $p(x_t | D_t)$ using the Monte Carlo approximation [2], [3]:

$$E[\hat{x}_t] = \frac{1}{N} \sum_{i=1}^N x_t^i \quad (41)$$

Where x_t^i is the i -th sample taken from $p(x_t | D_t)$. However, taking samples will be difficult – if not impossible, indeed, if $p(x_t | D_t)$ is a complex function, which is most likely the case. This process can be simplified by applying Importance Sampling [4], [5], which is the essential aspect of particle filters. The idea is as follows, we write Equation 40 as:

$$E_p[\hat{x}_t] = \int x_t p(x_t | D_t) \frac{q(x_t | D_t)}{q(x_t | D_t)} dx_t \quad (42)$$

Apparently, $q(x_t | D_t) / q(x_t | D_t)$ is one and it does not matter what it is. Yet it plays a significant role inside the integration, for now we can compute the expected value with respect to $q(x_t | D_t)$ as opposed to $p(x_t | D_t)$:

$$E_q[\hat{x}_t] = \int w_t x_t q(x_t | D_t) dx_t \quad (43)$$

where

$$w_t = \frac{p(x_t | D_t)}{q(x_t | D_t)} \quad (44)$$

so that,

$$E_p[\hat{x}_t] = E_q[w_t \hat{x}_t] \quad (45)$$

The significance of Equation 43 is this: We can choose a suitable $q(x_t | D_t)$ from which we can take N representative samples. Since we choose q , sampling should be possible¹. Once we have the samples, we can instantiate w_t^i by evaluating $p(x_t | D_t)$ for each x_t^i and use Monte Carlo approximation to

¹Having said this, q cannot be chosen arbitrarily. To begin with, both q and p should have the same domain. Secondly, q should be chosen in such a way that more samples are obtained from ‘important’ regions of p (in other words, p and q should be as similar as possible). Thirdly, p/q should be bounded. For more on this, we refer the reader to [5], [4], [6].

compute the expected value. The posterior probability itself can be approximated as follows:

$$p(x_t|D_t) = \sum_{i=1}^N w_t^i \delta(x_t - x_t^i) \quad (46)$$

where $\delta(x_t - x_t^i)$ is the Dirac delta function yielding everywhere zero except where $x_t = x_t^i$.

D. Sequential Importance Sampling

We wish to know whether it is possible to write Equation 44 recursively. Consider Equation 35. There, as in every Baye's expression, the denominator is a normalization factor and its significance is to ensure that the integration of the posterior distribution yields a unit area. This is one of the requirements of a valid probability density function. In our examination of the posterior distribution, we are mainly interested in making comparison of different probabilities signifying different possibilities, in which case we can ignore the normalization factor. Thus, the weight we attach to the t -th iteration during importance sampling can be expressed as:

$$w_t^i = \frac{p(X_{0:t}|D_t)}{q(X_{0:t}|D_t)} \quad (47)$$

Since the denominator can also be written as $q(x_t, X_{0:t-1}|D_t)$ using conditional probability, it can be expressed as:

$$q(X_{0:t}|D_t) = q(x_t|x_{t-1}, D_t) q(X_{0:t-1}|D_{t-1}) \quad (48)$$

This is because, the past state (location) of the robot does not depend on the future measurement, so that:

$$q(X_{0:t-1}|D_t) = q(X_{0:t-1}|D_{t-1})$$

Consequently, if we take the ratio of the numerator of Equation 35 and the above expression, the weigh we attach to the i -th sample of the t -th iteration, can be expressed as:

$$w_t^i = w_{t-1}^i \frac{p(z_t|x_t) p(x_t|x_{t-1})}{q(x_t|x_{t-1}, D_{t-1})} \quad (49)$$

Earlier we have asserted that we choose q during importance sampling. If we choose the denominator to be:

$$q(x_t|x_{t-1}, D_{t-1}) = p(x_t|x_{t-1}) \quad (50)$$

then, Equation 49 reduces to:

$$w_t^i = w_{t-1}^i p(z_t|x_t) \quad (51)$$

V. MODEL PARAMETERS

In Section IV we put the mathematical foundations of recursive estimation. In the literature some variants of these may exist, but the essential features remain the same. What distinguishes a particular indoor localization system from all other systems is mainly the underlying sensing setup and the way it establishes its model parameters (we shall give a review of these in Section VII). The latter is rather a crucial step because the estimation error depends on it to a great extent. Hence, besides the quality of the sensors, there should be adequate statistics to model the errors listed in Table I.



Fig. 1. Using a laser-based distance sensor as a reference to determine measurement statistics

The purpose of this section is to demonstrate how model parameters can be established. We employ two complementary sensing mechanisms to localize a mobile robot inside our lab. In the first, we use an inertial measurement unit consisting of a 3D accelerometer and a 3D gyroscope. The second setup consists of four static ultra-wide band (UWB) sensor nodes attached on the four walls of the lab and an additional node carried by the mobile robot. The static nodes periodically emit beacons and the mobile node calculates the difference in the time-of-arrival [7] of these beacons to determine its relative location in the room. As a reference system to measure the actual location of the robot, we employ a Bosch laser-based distance measuring device having an accuracy of ± 1.5 mm, as shown in Fig. 1 in both cases.

A. Process Error

The process error, which is an inherent aspect of the driving setup of the robot, is independent of the underlying sensing infrastructure. To obtain the statistics of this error we conditioned the robot to move in a straight line (along the x-axis) and at a constant velocity between two sampling (decision) intervals (ref. to Fig. 2). A deviation from this path in the y-axis and a deviation in the distance traveled in a fixed time along the x-axis constitute the process error statistics, e_p . The process error varies with the speed of the robot and the distance it traveled. Hence, in order to establish representative statistics, one needs to repeat the experiment several times, considering different speed and distance. The speed of our robot can vary from 0.5 to 1.2 m s^{-1} . We varied the robot's speed at 0.2 m s^{-1} interval and for each configuration we repeated the experiment twenty times. We then merge the data from all the experiments to establish the process error statistics. Fig. 3 displays the resulting process error statistics for one of the dimensions (the x-axis, the primary dimension of movement).

B. Transition Probability Density Function

One of the strengths of the Bayesian Estimation (Equation 35) is its inclusion of the transition probability density.

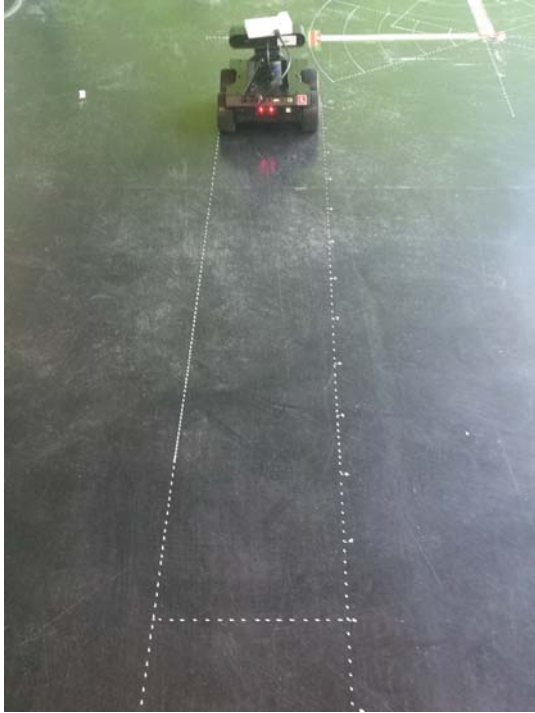


Fig. 2. The setup for establishing the process error.

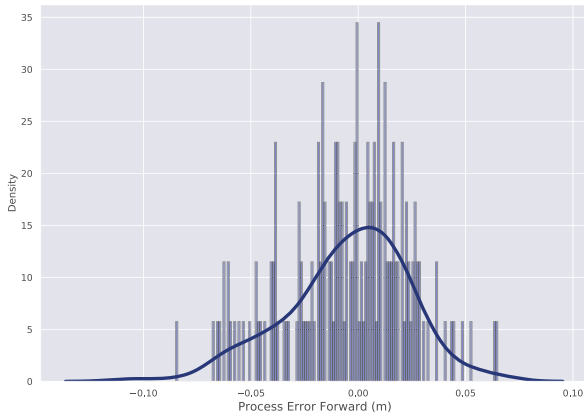


Fig. 3. The forward movement (x-axis) process error statistics.

Theoretically, it is the prediction component of the estimation. Practically, however, its implementation as well as application is not always straightforward. This is because the uncertainty in the present location of the robot arises from the uncertainty associated with not only its past location but also the speed with which it traveled in the time interval $[t-1, t] - p(x_t|x_{t-1}, v_{t-1})$. On the other hand, the transition probability connects only the present and the past locations, $p(x_t|x_{t-1})$. This said, once a decision is made as regards the robot's location at $t-1$, then the uncertainty associated with its location at t is a function of the uncertainty associated with the speed of travel, in which case, this uncertainty reduces to e_r , which is the process error.

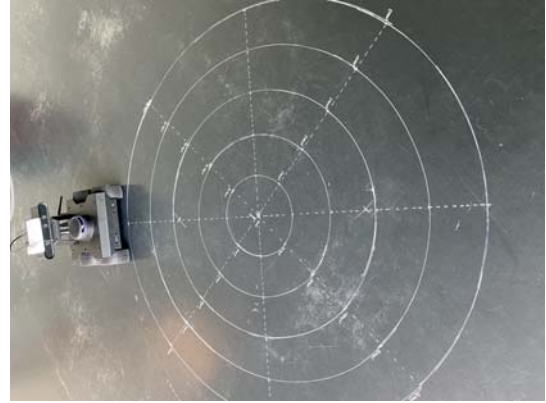


Fig. 4. Establishing the measurement and prediction statistics of inertial measurement units using a polar coordinate system.

C. Inertial Measurement Units

The employment of a 3D gyroscope and a 3D accelerometer enables to measure linear displacement and angular accelerations (turns) simultaneously. This, in turn, simplifies the mapping of a moving (local) frame of reference onto a static (global) frame of reference. The static frame of reference can be rectangular (Cartesian) or polar, but we chose a polar frame of reference, as shown in Fig. 4, because it is easier to model the measurement error. The radius of the most outer circle in Fig. 4 is 0.5 m. If the robot sets off from the most outer circle and travels in a straight line, it should have traveled 0.5 m by the time it reaches at the center. When at the center, the position of the robot is estimated by evaluating the acceleration reading (the difference in time between points of acceleration -when the robot sets off- and deceleration -when the robot arrives at the center- of the IMU). To obtain the measurement statistics of the gyroscope, at the center, the robot follows one of the dashed lines to travel to the outer circle. The measurement error is the difference between the actual angle and the angle read by the gyroscope. Figure 5 show the measurement errors statistics established this way for the accelerometer and the gyroscope. As can be seen, the accelerometer introduces a significant uncertainty.

D. Ultra-Wide Band Radio

The accuracy of the UWB radio greatly depends on the location of the robot with respect to the anchor nodes. Therefore, in order to establish sufficient statistics, sample points representing the dimension of the entire area of mobility should be selected and repeated measurement should be taken from each point. Our lab has a dimension of $8.692 \times 5.866 \text{ m}^2$. We identified $5 \times 5 = 25$ such points and took 100 measurements from each point. Fig. 6 shows the measurement statistics we established accordingly. The statistics suggest a normally distributed measurement error, but the density is not centered at zero, as can be seen.

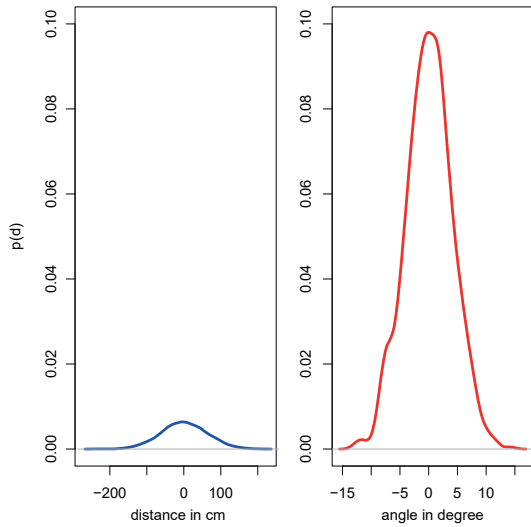


Fig. 5. Estimated measurement error statistics corresponding to the linear and angular accelerations.

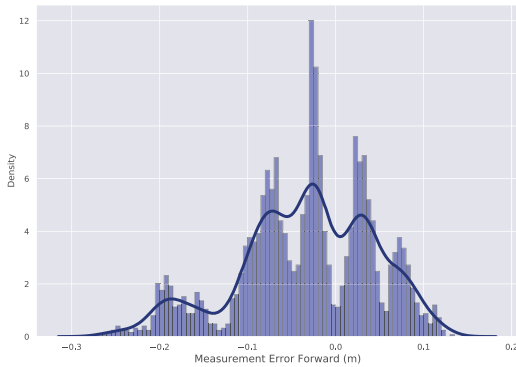


Fig. 6. The measurement error statistics (x-axis, in meter) corresponding to the UWB setup.



Fig. 7. The trajectory for a mobile robot in a polar coordinate system for self-navigation.

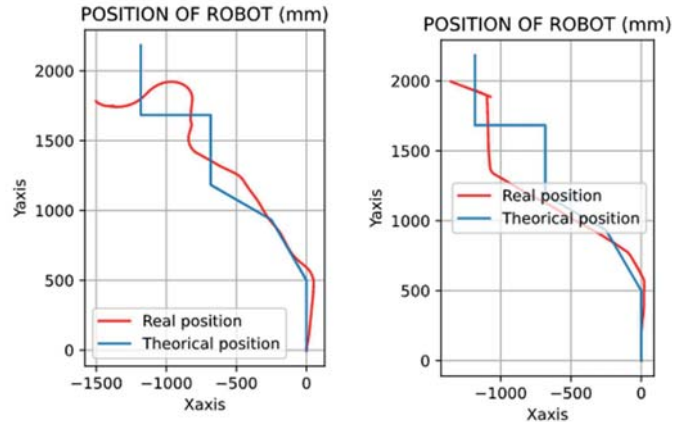


Fig. 8. The actual (ideal) and real (estimated) trajectories of the mobile robot. The real trajectory was established using a Kalman Filter.

VI. SELF-NAVIGATION

The model parameters we established in the previous section suggest that the process and measurement errors statistics have normal distributions. Hence, with the proper calibration of the parameters, it is possible to employ the kalman filter to self-localize the robot in our lab. In this section, we illustrate how we employed the IMU setup to estimate the trajectory (Fig. 7) along which the mobile robot navigated. The robot self-navigated using a QR code scanner. In parallel, the kalman filter estimated the trajectory. In order to reduce the accumulation of error during the conversion of the linear acceleration to position, the IMU was reset between any two decision (sampling) points. We considered two different values for the speed of the robot: In the first –Fig. 8 (left) – the robot was moving at a velocity of 1 m s^{-1} whereas in the second (right), it was moving at 0.5 m s^{-1} , since during the setup of the model parameters, we have observed that fast movements are better for estimation than slow movements. This is because differentiating between the noise arising outside of the estimation setup and the error inherent to it is easier when there is a distinct acceleration. This observation seem to be consistent Fig. 8.

VII. RELATED WORK

In the past decade, several researchers have attempted to employ a plethora of freely available sources for indoor localization. In [8], the authors noted that modern WiFi Network Interface Cards (NICs), such as the Intel Link 5300, provide multiple antennas and a rich set of Channel State Information for each received packet (up to 30 distinct CSI can be extracted from OFDM-based WiFi setting from each antenna). The authors apply this information to a fine-grained indoor localization using offline fingerprinting. A neural network with four hidden layers is used to train the system, and a probabilistic online algorithm is used for mapping the outputs of the three antennas to a location on a two-dimensional map. The authors tested their prototype in a living room and a university lab to

report remarkable results (achieving an estimation accuracy of less than 1 m in certain places).

In [9], the authors exploit the richness of bandwidth and high bit rate in UWB settings to localize nodes. The proposed approach employs Differentiated Time-of-Arrival (DTOA) [10] and consists of three types of nodes: anchor nodes, a reference node, and a Tag. The latter is a node whose location is unknown and to be determined. The reference node and the anchor nodes, which are located at static and known positions, coordinate packet transmission, so that the Tag node can apply DTOA to localize its position. Thus, first the reference node sends an INIT message, thereby triggering the anchor nodes to respond with a RESP message after a predefined delay. The delay time has two components: a common delay component, ΔR , and an anchor specific component, δ_n . The latter, in the range of nanoseconds, is introduced to ensure that collision does not occur on the RESP packets. Furthermore, it has the additional benefit of identifying responses and discerning them from strong multi-path effects.

In [11], the authors combine time-difference-of-arrival with spectral discrimination to localize a node in the presence of multi-path scattering and shadowing. A node broadcasts a packet to multiple access points, each of which calculates the time-of-arrival to produce a local hyperbolic locus. Moreover, in order to remove the effect of multi-path scattering and non-line-of-sight transmission, it analyzes the spectral characteristics of the received packet and either filters the dominant component (suggesting line-of-sight) or combines multiple dominant components to compensate for multi-path travel time. Finally, it transmits the local hyperbolic locus back to the node. The mobile node calculates the difference in distance to estimate its position. The authors report an estimation accuracy of below 90 cm in an office environment using 4 access points. The authors also claim that the proposed approach was robust to signal shadowing, even in the presence of a wall standing between the access points and a mobile node. The proposed approach works well in an UWB Wi-Fi environment in order to enable fine-grained estimation of time-of-arrival and to obtain sufficient spectral insight in a very short time.

In [12], the authors combine fingerprinting with an inertial calibration system for a 3D indoor localization. The fingerprinting is based on the evaluation of Bluetooth Low Energy (BLE) beacons. The proposed approach, which employs particle filters, assigns a probability to each particle at time t conditioned by the decision made at time $t-1$ and the signal strength of a local reference signal for the time t . An internal state machine continuously monitors the consistency of the fingerprinting outcomes with an inference made by the inertial system. The outcomes of the inertial system are, in turn, combined with the outcomes of a barometric pressure sensor to infer upward and downward movements, which is the basis for 3D localization. A maximum likelihood estimate combines the outputs of the three sources, namely, the BLE beacons, the inertial sensors, and the barometric pressure sensor, to estimate the most likely location of a smartphone.

The proposed approach was tested inside a 21000 square metre mall by visually impaired shoppers who could freely navigate the mall using a prototype implementation.

In [13], the authors fuse information from a magnetometer sensor, a gyroscope, and a WiFi using an augmented particle filter. The samples taken from these sources form vectors which are then mapped to a probability distribution on the basis of which the value of a particle is estimated. The particles, which correspond to pixels in a 2D map, in turn, signify a step, the length of a step, a direction, or a turn. Finally, the values of the particles are compared with offline-produced fingerprints. The proposed approach was tested in various locations: supermarket, parking garage, and office. The authors claim to have achieved an impressive accuracy for each place and for each combination of sources, but the paper also withholds vital information as regards the actual features extracted from the sensors, the mapping from the raw data to the probability distribution, the connection between the features and the higher-level contexts, and the specific steps taken to produce the offline fingerprints.

Indoor localization based on Inertial Measurement Units (IMUs) – i.e., 3D accelerometers, 3D gyroscope, and 3D magnetometers – belongs to the most popular approaches, because it requires minimum infrastructural support and is relatively robust to environmental dynamics. A significant portion of the proposed approaches focuses on localizing human beings using smartphones [14], though interest in localizing mobile robots is also growing.

In [15], the authors employ a particle filter to estimate the current walking length and direction of a person based on several input parameters: RSSI values from a WiFi access point, samples of IMU, and knowledge of the previous position (dead reckoning). These inputs are used to generate weighted “particles” on the basis of which the posterior distribution of the whereabouts of the person is estimated. Occasionally, the filter calibrates itself using strategically placed beacons. The authors tested their model in a big building complex at Berkeley campus, University of California, and reported remarkable results (an estimation accuracy in the order of tens of centimeters).

Indoor localization of mobile robots, in addition to IMUs, can take advantage of several locally available sensors including 3d cameras, depth and proximity sensors (laser, infrared, and ultrasound), and QR code scanners [16]. Thus, in [17], the authors employ data from a thermal camera (long-wave infrared camera) and IMU to set up an extended Kalman filter which performs an odometer estimation. In [18], the authors express indoor localization as an optimization problem. A combination of odometer and gyroscope data describe the independent variables (the measurements) and position and heading, the dependent variables. The optimization problem is solved using extended H_∞ . Sporadically available QR code scanners are used to fine-tune model parameters and as a feedback mechanism.

VIII. CONCLUSION

In this paper we closely examined the scope and usefulness of recursive estimation in indoor localization of mobile robots. We discussed the different types of errors and the assumptions guiding the estimation assignment. Any estimation assignment has two goals, namely, (1) to align the *mean* of the estimated random variable with the *actual* location of the robot; and (2) to minimize the *variance* of the estimated random variable (our uncertainty). We showed that recursive estimation techniques combine prediction and measurement components. In a kalman filter, the prediction component is expressed in abstract, whereas in a Bayesian Estimation and a particle filter, it is concrete, being expressed as a transition probability, $p(x_t|x_{t-1})$. Yet we also showed that the transition probability often arises from the error in the driving setup of the robot which is encoded as a process error in the Kalman filter formulation.

We highlighted that whether or not an estimation assignment is successful greatly depends on the model parameters and the adequacy of the statistics which represent them. We demonstrated how process, measurement, and prediction statistics can be established for two different sensing setups: Inertial Measurement Units (IMU) and ultra-wide-band technology (UWB).

In this paper we have not quantitatively evaluated the overall navigation error. Our next goal will be to do this for different configurations: a kalman filter with IMU vs UWB setup; a particle filter with IMU vs UWB setup; and a 2D navigation vs a 3D navigation.

REFERENCES

- [1] R. E. Kalman, "A new approach to linear filtering and prediction problems," *Transactions of the ASME—Journal of Basic Engineering*, vol. 82, no. Series D, pp. 35–45, 1960.
- [2] K. Binder, D. Heermann, L. Roelofs, A. J. Mallinckrodt, and S. McKay, "Monte carlo simulation in statistical physics," *Computers in Physics*, vol. 7, no. 2, pp. 156–157, 1993.
- [3] E. Zio, "Monte carlo simulation: The method," in *The Monte Carlo simulation method for system reliability and risk analysis*. Springer, 2013, pp. 19–58.
- [4] R. M. Neal, "Annealed importance sampling," *Statistics and computing*, vol. 11, no. 2, pp. 125–139, 2001.
- [5] M. F. Bugallo, V. Elvira, L. Martino, D. Luengo, J. Miguez, and P. M. Djuric, "Adaptive importance sampling: The past, the present, and the future," *IEEE Signal Processing Magazine*, vol. 34, no. 4, pp. 60–79, 2017.
- [6] I. Papaioannou, K. Breitung, and D. Straub, "Reliability sensitivity estimation with sequential importance sampling," *Structural Safety*, vol. 75, pp. 24–34, 2018.
- [7] C. Falsi, D. Dardari, L. Mucchi, and M. Z. Win, "Time of arrival estimation for uwb localizers in realistic environments," *EURASIP Journal on Advances in Signal Processing*, vol. 2006, pp. 1–13, 2006.
- [8] Y. Shu, C. Bo, G. Shen, C. Zhao, L. Li, and F. Zhao, "Magical: Indoor Localization Using Pervasive Magnetic Field and Opportunistic WiFi Sensing," *IEEE Journal on Selected Areas in Communications*, vol. 33, no. 7, pp. 1443–1457, Jul. 2015.
- [9] B. Großwindhager, M. Stocker, M. Rath, C. A. Boano, and K. Römer, "SnapLoc: An Ultra-Fast UWB-Based Indoor Localization System for an Unlimited Number of Tags," in *Proceedings of the 18th International Conference on Information Processing in Sensor Networks - IPSN '19*. Montreal, Canada: ACM Press, Apr. 2019.
- [10] X. Li, Z. D. Deng, L. T. Rauchenstein, and T. J. Carlson, "Contributed Review: Source-localization Algorithms and Applications Using Time of Arrival and Time Difference of Arrival Measurements," *Review of Scientific Instruments*, vol. 87, no. 4, Apr. 2016.
- [11] J. Xiong, K. Sundaresan, and K. Jamieson, "ToneTrack: Leveraging Frequency-Agile Radios for Time-Based Indoor Wireless Localization," in *Proceedings of the 21st Annual International Conference on Mobile Computing and Networking - MobiCom '15*. Paris, France: ACM Press, Sep. 2015.
- [12] M. Murata, D. Ahmetovic, D. Sato, H. Takagi, K. M. Kitani, and C. Asakawa, "Smartphone-based Indoor Localization for Blind Navigation across Building Complexes," in *2018 IEEE International Conference on Pervasive Computing and Communications (PerCom)*. Athens, Greece: IEEE, Mar. 2018.
- [13] X. Wang, L. Gao, S. Mao, and S. Pandey, "CSI-based Fingerprinting for Indoor Localization: A Deep Learning Approach," *IEEE Transactions on Vehicular Technology*, vol. 66, no. 1, pp. 763–776, Jan. 2016.
- [14] F. Zafari, A. Gkelias, and K. K. Leung, "A survey of indoor localization systems and technologies," *IEEE Communications Surveys & Tutorials*, vol. 21, no. 3, pp. 2568–2599, 2019.
- [15] H. Zou, Z. Chen, H. Jiang, L. Xie, and C. Spanos, "Accurate indoor localization and tracking using mobile phone inertial sensors, wifi and ibeacon," in *2017 IEEE International Symposium on Inertial Sensors and Systems (INERTIAL)*. IEEE, 2017, pp. 1–4.
- [16] R. Karlsson and F. Gustafsson, "The future of automotive localization algorithms: Available, reliable, and scalable localization: Anywhere and anytime," *IEEE signal processing magazine*, vol. 34, no. 2, pp. 60–69, 2017.
- [17] C. Papachristos, F. Mascarich, and K. Alexis, "Thermal-inertial localization for autonomous navigation of aerial robots through obscurants," in *2018 International Conference on Unmanned Aircraft Systems (ICUAS)*. IEEE, 2018, pp. 394–399.
- [18] P. Nazemzadeh, D. Fontanelli, D. Macii, and L. Palopoli, "Indoor localization of mobile robots through qr code detection and dead reckoning data fusion," *IEEE/ASME Transactions on Mechatronics*, vol. 22, no. 6, pp. 2588–2599, 2017.